coatings

MDPI

Article

Influence of Oil Palm Nano Filler on Interlaminar Shear and Dynamic Mechanical Properties of Flax/Epoxy-Based Hybrid Nanocomposites under Cryogenic Condition

Natrayan Lakshmaiya [1], Seeniappan Kaliappan [2], Pravin P. Patil [3], Velmurugan Ganesan [4], Joshuva Arockia Dhanraj [5], Chattariya Sirisamphanwong [6], Tanakorn Wongwuttanasatian [7,8], Shahariar Chowdhury [9,*], Sittiporn Channumsin [10,*], Manun Channumsin [11] and Kuaanan Techato [9]

1 Department of Mechanical Engineering, Saveetha School of Engineering, SIMATS, Chennai 600124, India
2 Department of Mechanical Engineering, Velammal Institute of Technology, Chennai 601204, India
3 Department of Mechanical Engineering, Graphic Era Deemed to be University, Bell Road, Clement Town, Dehradun 248002, India
4 Institute of Agricultural Engineering, Saveetha School of Engineering, SIMATS, Chennai 600124, India
5 Center for Automation & Robotics (ANRO), Department of Mechatronics Engineering, Hindustan Institute of Technology and Science, Chennai 603103, India
6 Department of Physics and General Science, Faculty of Science, Nakhon Sawan Rajabhat University, Nakhon Sawan 60000, Thailand
7 Center for Alternative Energy Research and Development, Khon Kaen University, Khon Kaen 40002, Thailand
8 Mechanical Engineering Division, Faculty of Engineering, Khon Kaen University, Khon Kaen 40002, Thailand
9 Faculty of Environmental Management, Prince of Songkla University, Hatyai 90110, Thailand
10 Space Technology Research Center, Geo-Informatics and Space Technology Development Agency (GISTDA), Chonburi 20230, Thailand
11 Faculty of Veterinary Medicine, Rajamangala University of Technology Tawan-Ok, Chonburi 20110, Thailand
* Correspondence: mdshahariar.c@psu.ac.th (S.C.); sittiporn@gistda.or.th (S.C.)

check for updates

Citation: Lakshmaiya, N.; Kaliappan, S.; Patil, P.P.; Ganesan, V.; Dhanraj, J.A.; Sirisamphanwong, C.; Wongwuttanasatian, T.; Chowdhury, S.; Channumsin, S.; Channumsin, M.; et al. Influence of Oil Palm Nano Filler on Interlaminar Shear and Dynamic Mechanical Properties of Flax/Epoxy-Based Hybrid Nanocomposites under Cryogenic Condition. *Coatings* **2022**, *12*, 1675. https://doi.org/10.3390/coatings12111675

Academic Editor: Günter Motz

Received: 12 October 2022
Accepted: 25 October 2022
Published: 4 November 2022

Abstract: Natural fiber-reinforced polymer composites are gaining in popularity due to recyclability and availability. This research investigates how oil palm shell (OPS) filler materials impact the interlaminar shear and the dynamic properties of flax fiber-reinforced hybrid composites under cryogenic circumstances. Filler materials in two different proportions (0, 2, 4, and 6 wt.% OPS) and 40 wt.% flax fibers were used to make composites. The OPS filler-filled polymeric materials were invented through typical hand lay-up. The hybrid materials were imperiled to liquid nitrogen for varying amounts of time after production (15 and 30 min). According to the findings, OPS nanoparticles can be used as natural rather than artificial fillers. Furthermore, loading 4 wt.% OPS nanoparticles into organic fabric-strengthened epoxy polymeric materials during 15 min of cryogenic settings resulted in the best interlaminar shear and dynamic performances. The storage and loss modulus of the flax/epoxy composites were improved by adding a 4% OPS nanofiller. The improvement can be ascribed to the hardness and stiffness of the additional OPS nanofillers. The 4% nano-OPS/flax/epoxy hybrid nanocomposite's damping factor was substantially reduced compared to the flax/epoxy composites. The OPS nanofiller limits the epoxy molecular chain's free segmental mobility, resulting in a lower damping factor and enhancing the adherence among flax fibers and the epoxy resin. The shattered specimen of the hybrid materials was investigated using a scanning electron microscope.

Keywords: flax fiber; OPS filler; nano hybrid composites; interlaminar shear strength; dynamic mechanical properties; cryogenic treatment

1. Introduction

A composite material is a material that is produced from two or more constituent materials. These constituent materials have notably different chemical or physical properties and are merged to create a material with properties unlike the individual elements [1].

Natural fibers as a reinforcement in polymeric materials have sparked a lot of attention due to rising recognition of the importance of a green and more nurturing environment in the population. Various reprocessing and sustainable energy waste materials such as waste newspaper, woody biomass, reservoir slit, waste concrete, and others have been successfully used in plaster or polymers to replace highly-priced raw materials such as cement blocks and concrete in prefabrication and construction uses [2,3]. As a result, the need for essential resources, waste management, and environmental implications are reduced. Compared to standard composite applications, natural fiber-reinforced composite materials have several benefits and drawbacks [4]. The thermal and mechanical characteristics of the composites were lowered due to defects such as poor soaking and poor interfacial adhesion. However, these drawbacks may be remedied by modifying the fibers with physical or chemical treatment or by introducing interface preservatives [5]. The interface additions can be nanofillers (TiO_2, SiO_2, nano clay) or synthetic fabric (carbon fibers, glass fibers) to make hybrid composites by correct material design. Many factors influence the characteristics of these composite samples such as the resin type, fiber dimensions, nanofiller type, bonding strength between fibers or fillers and matrices, etc. [6].

Hybrid composites are gaining a lot of interest as sophisticated structural and engineering materials that mix economic effectiveness and productivity well. Hybrid materials are fashioned by combining two or more distinct types of fibers in a similar manner or reinforcements in blends. They have an extensive assortment of possible submissions in structural, semi-structural, and non-structural industrial applications [7,8]. Nanomaterials are multiphase densely composite materials with one, two, or three dimensions of less than 1 m in at least one stage [9]. Incorporating the nanoscale additives into the polymer matrices fulfil the demands for unique characteristics in various manufacturing and practical applications. Nanocomposites are among the most potential, appealing, necessary, and inspiring topics in prospective industrial applications [10]. Nanomaterials outperform pure polymers and even conventional materials such as glass fiber-reinforced composites in terms of physical, mechanical, thermodynamic, chemical, electromagnetic, and barrier characteristics. Flaxseed (*Linum usitatissimum* L.) seems to be the only agriculturally significant species in the *Linaceae* category, encompassing twelve groups of approximately 400 species [11]. Flaxseed was the first cereal used to make cloth and harden it into matrices, and it was discovered in European graves around 5000 B.C. This represents one of the most widely used spores. Flaxseed has grown for generations for its textiles and oils, making it a significant product. Flaxseed seems to be the subject of intensive research and the development of desired features such as herbicide resistance, resistance to biogenic stressors, and better oils and fiber qualities [12,13].

Hybrid nanomaterials have revolutionized materials research by showing the most cutting-edge modern composites. Due to excellent distribution, high aspect ratios, and efficient polymeric filler contact, the inclusion of nanostructures significantly improves the thermal, physiological, dynamic, and mechanical characteristics [14,15]. The most suitable and cost-effective precursors for manufacturing nanostructures or fillers are currently lignocellulosic and agricultural production-based on renewable sources. Many researchers have reported on sawdust, sugarcane waste, cellulose nanofibers from rubber wood, CSP, rice husk, and coir pith powder [16,17]. Due to their high yield strength, max hardness, and high density, nanomaterial additives and tidal silicate minerals such as montmorillonite and naturally altered montmorillonite nano clay are presently gaining more consideration since they can change the physical, thermal, and mechanical properties of natural composite materials [18,19].

Nanoparticles would provide the matrix with a huge superficial zone due to their small size. However, using artificial fillers in polymer composites is problematic due to the difficulty of ensuring the homogeneous spread of inorganic fillers in the polymeric resins. Inorganic nanoparticles have a propensity toward clumping together [20]. As a result, using artificial nanoparticles as an additive may cause the composite to deteriorate, lowering the material characteristics of the polymeric composites. Furthermore, synthetic fibers are an environmental problem and a health threat for those working in the composites manufacturing industry [21]. Due to their ecologically benign character, cellulosic materials have been used as a substitute for traditional fibers in the production of polymeric composites in recent years. However, there are several drawbacks to using lignocellulosic biomass in fiber-reinforced polymer composites such as standard reinforcement/resin interfaces, moisture struggle, and reduced toughness [22]. Because of the poor bonding connections between the matrix and the fibers, the composite's physical, thermal, and mechanical characteristics may suffer significantly. The inclusion of nanoparticles into the fiber matrix is one of the ways that might be used to address the lack of natural fiber matrix compatibility [23]. Oil palm shells (OPSs) are a lignocellulosic material considered as agricultural waste. In the plantation region, OPS is usually burnt or utilized as a covering on the top of roadways. In contrast, using nanoparticles in a fiber-based matrix can potentially improve and enhance the capabilities. Cryogenic properties can improve the mechanical characteristics of fiber-reinforced composites. Aircraft metals, for instance, must be capable of coping with temperatures as high as 200 °C [24]. Cryogenically treated and polymeric materials have substantially improved toughness, rigidity, and fracture toughness. As a consequence, compressed gas hybrids could still be a significant part of ongoing design and technology to increase the organic polymeric properties.

The influence of a newly designed nanofiller on the interlaminar shear and dynamic mechanical characteristics of flax fiber reinforced epoxy under cryogenic conditions was investigated in this research. The current research entails the creation of a nanofiller from oil palm empty fruit bunch fibers using a ball milling process. The hand lay-up approach creates pure flax epoxy composites and flax hybrid nanocomposites.

2. Experimental Procedure

2.1. Materials

Rithu Fiber Industry provided the woven flax fiber mat utilized in this study in Madurai, Tamilnadu, India. The OPS chips were provided by the Raju palm oil plant in Chennai, Tamil Nadu, India. Rithu Chemical Industry, Chennai, Tamil Nadu, India offered the epoxy Araldite AW 206 and HV 953 hardener. The braided flax fiber was cleansed adequately with distilled water before drying in an oven at 73 °C. Finally, the fibers were soaked for 4 h in 5% NaOH solutions to remove impurities and other pollutants from the water molecules. Figure 1 shows the OPS nanofiller extraction procedure from palm trees.

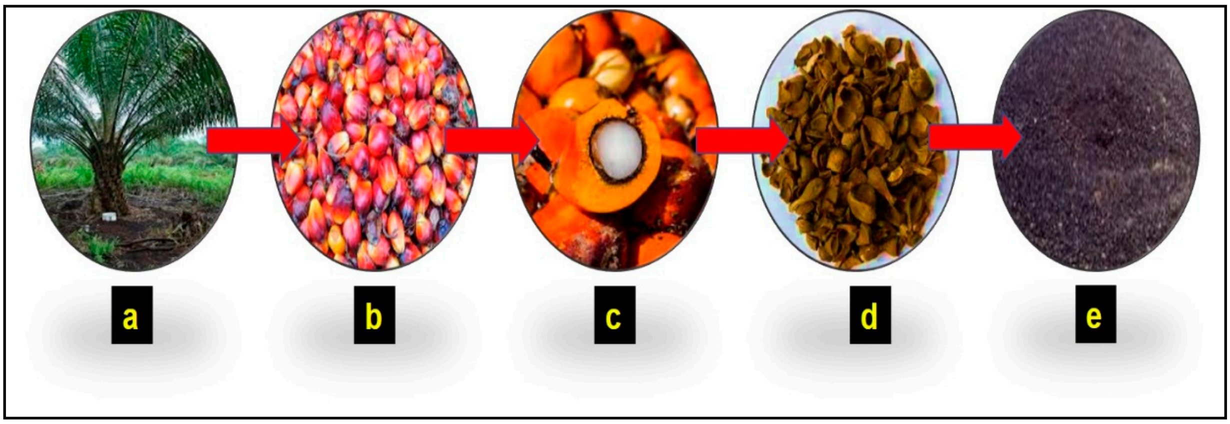

Figure 1. Extractions of OPS particles from palm tree. (**a**) Palm tree; (**b**) fruit; (**c**) kernel; (**d**) shell; (**e**) OPS filler.

2.2. Formation of OPS Nanofiller

OPSs were transformed into granular particles by crushing the gathered palm shell fries in a ball mill. Following this, the OPS granules were filtered to remove the under-sized particles from the mill (e.g., microparticles, gravel, and sand). To minimize the moisture content of the filtered palm shells, they remained dehydrated in the oven for 30 h at 120 °C. The ground dry OPS granular material was filtered to 1–1.5 mm. The refined OPS residue was further processed using a high-energy ball mill at 180 revolutions per minute for 20 h. The specimens were oven dried for 48 h at 120 °C to minimize aggregation and moisture interaction.

2.3. Composite Fabrications

The natural hybrid composites were fabricated through manual lay-up procedures to keep the total fiber loading of flax fibers at 40 wt.%. The palm shell nanofiller/epoxy matrix was created by dissolving palm shell particles (2–6 wt.%) in an epoxy matrix and mixing for 20 min at 250 rpm with a mechanical stirrer before adding the hardener. The hybrid composites were then submerged in an OPS nanofiller/epoxy matrix until the fibers were liquefied. The fiber mats were soaked in a stainless-steel mold with 150 mm × 150 mm × 3 mm sizes. The molds were then closed for a warm press at 150 psi, followed by 24-h curing at ambient temperature. As a control, a clean hybrid laminate without fillers was made. After fabrication, the composite plates were cut as per the ASTM standard.

2.4. Cryogenic Treatment

The cryogenic treatments were performed in a heat-manipulated cryogenic chamber using pre-programmed electronics. The temperature was lowered to −196 °C using a controlled frequency of chilling (3 °C/min). Following the design of experiments, the prototypes were again submerged in liquid N_2 at −196 °C for low-temperature processing for various periods.

2.5. Characterization of Hybrid Composites

A Shimadzu (AGS-10 kNG type, Chennai, India) Universal Testing Machine was used to assess the nanocomposites' interlaminar shear strength (ILSS). The ASTM 2344-84 requirements were followed for this test, and the specimen span length was kept at 16 mm. The crosshead speed was kept constant at 2 mm/min. Three specimens were tested in each case, and the average value was calculated. This is a three-pointed short-beam approach. Nonlinear finite element modeling was employed to assess the elasticity characteristics of the nanomaterial following ASTM D4065-01. The DMA approach determines the viscoelastic behavior of nano-based epoxy composites (storage modulus, loss modulus, and damping factor). Model DMS 6100 was used to evaluate the DMA performance with weights of OPS-added flax fiber epoxy composites (Nano Technology Research Center, Sathiyabama University, Chennai, India). The samples for the DMA test were machined to ASTM standard D 4065 dimensions of 55 mm × 13.5 mm × 3 mm. The experiments were carried out in a nitrogen atmosphere using the three-point bending mode at a constant frequency of 1 Hz. The temperature range was increased from 30 to 200 °C at a rate of 5 °C/min. Three specimens were tested in each case, and the average value was calculated based on these conditions; the graphs were plotted. Equation (1) was used to calculate the fillers' effectiveness coefficients (*C*). S_g and S_r are the storage modules values in the glassy and rubbery regions.

$$C = \frac{S_g/S_r \text{ (Composites)}}{S_g/S_r \text{ (Resin)}} \tag{1}$$

3. Result and Discussion

3.1. Characterization of OPS Nanofillers

The particle size of the OPS nanoparticles was determined using X-ray diffraction (XRD, Rigaku Analytical Devices, Inc., Wilmington, NC, USA). The distribution of particle sizes of OPS was measured using a MALVERN Zettaliter (Master Sizer 3000, SRM University, Tamil Nadu, India) and a 532 nm laser. To guarantee the correctness of the findings, the tests were repeated three times. X-ray diffraction (XRD) was performed using a ULVAC-PHI5000 Probe III X-pert diffractometer (Rigaku Analytical Devices, Inc., Wilmington, NC, USA) with Cu-Ka1 radiation at 45 kV, 30 Ma, and λ = 1.54. At room temperature, the diffractograms were scanned from 10° to 80° (2 θ) at a scanning rate of 0.5° min^{-1}.

A tiny quantity of oil was found in the OPS after solvent extraction of the remaining oil from OPS nanoparticles. Utilizing n-hexane at 80 °C for 90 min, 1.7% of palm oil was recovered from the OPS nanomaterials. Figure 2 depicts the particle size distribution of the OPS nanomaterials by intensity, which spans a huge spectrum of nanoparticles with symmetrically curved behavior. The overall diameter of the majority of the particles varied from 51.23 to 92.2 nm, covering 80% of the nanoparticles. As a consequence, the results confirmed that the particles were nanosized. These particle size changes occurred during the ball milling process showed in Figure 2.

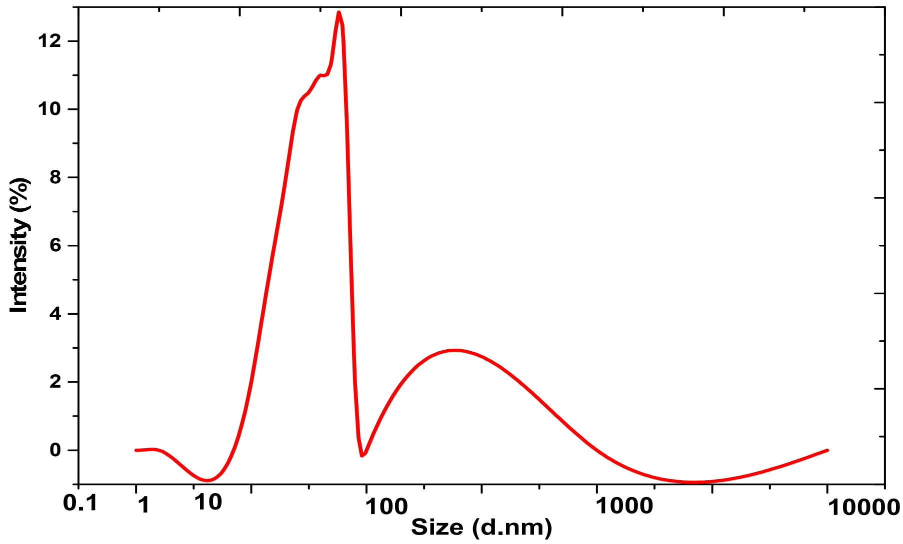

Figure 2. Particle size distribution of the OPS nanoparticles.

According to the investigation, the size of the OPS nanoparticles spanned between 10 and 30 nm, with irregular round forms, suggesting its nanometric character. The investigation further indicates that no aggregation of OPS nanoparticles occurred following extraction. Scherrer's equation calculated the average crystallite size from the X-ray diffraction peaks. Figure 3 shows the XRD pattern of the nanoparticles.

$$\mathrm{D} = \frac{K\,\lambda}{\beta cos\theta} \tag{2}$$

where D is the crystallite diameter; λ is the X-ray wavelength; β is the full width at half maximum of the diffraction peak; θ is the diffraction angle, and K is the Scherrer's constant of the order of unity for usual crystals. As shown in Figure 3, the reflecting peak at 2θ = 22.31°, 22.65°, and 22.98° were used to estimate the size of the OPS nanoparticles, resulting in a particle size of 41.32, 31.25, and 30.25 nm, respectively. The average size of the OPS nanoparticles was 34.273 nm.

Influence of the Nanoparticle Shape

Images from a transmission electron microscope (TEM) were collected to analyze the shape and morphology of the OPS nanoparticles. A 150-CX TEM (Rigaku Analytical Devices, Inc., Wilmington, NC, USA) at 100 kV was used to scan the samples at random. According to the TEM picture, the nanomaterial forms comprised spheres and triglycerides in the 10 to 500 nm range. According to Figure 4a,b, most of the nanoparticles were spherical in form. It was also validated by the XRD (Figure 3) picture. The peak line intensity was highest in the areas around 22° to 23°, as opposed to 50° to 80°. This might be due to the collection of comparable-shaped particles in that area. Particle form is another important physical factor influencing the nano-biomaterial–cell interaction. The form of a particle determines its uptake, distribution, and biological activities. In comparison to spherical nanoparticles, elongated nanoparticles have a greater uptake due to their ability to bind to the cells efficiently. This seems to be due to the curved lines of spherical particles having fewer binding sites to engage with the cell membrane [25]. On the other hand, extended nanocrystals have a more excellent surface area-to-volume ratio, ensuring efficient contact with the cell surface. Sharp-shaped nanostructures, in general, may puncture cell walls and efficiently internalize them. The exocytosis of high aspect ratio particles was lower than that of the spherical nanoparticles. However, opposing internalization trends were observed for spherical OPS nanoparticles and subsequent dynamically distorted quasi-ellipsoidal nanomaterials with distinct dimensions. Cylindrical nanoparticles were more readily absorbed than the non-spherical equivalents [26]. The sphere-shaped OPS particles aid in boosting the ILSS behaviors of the composite due to the high surface areas.

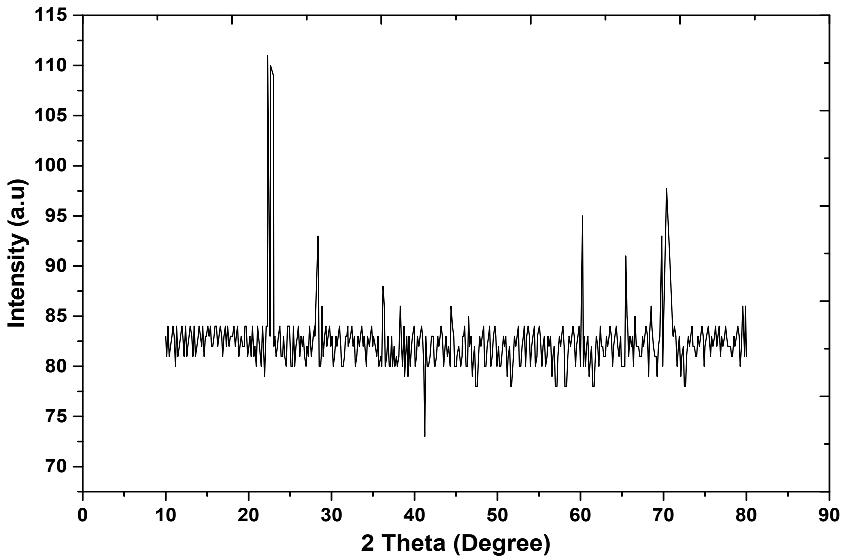

Figure 3. XRD pattern of the OPS nanoparticles.

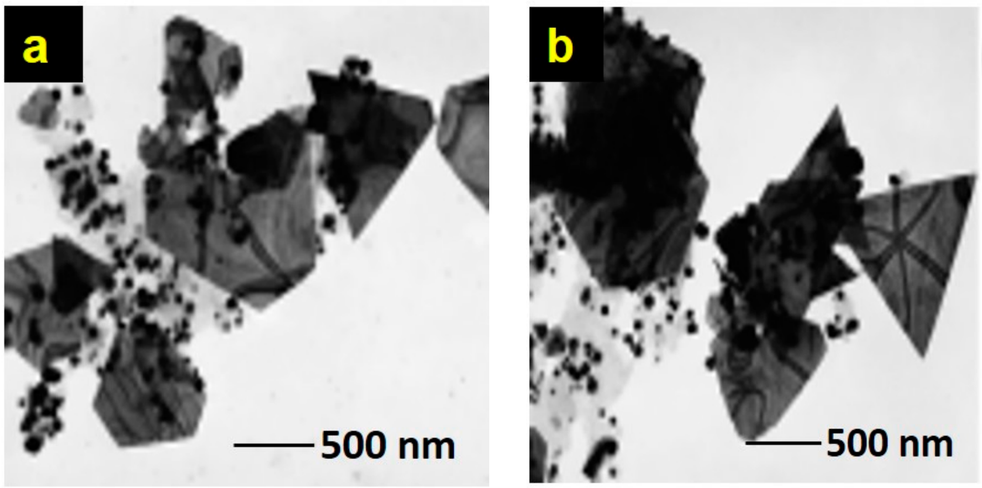

Figure 4. (**a**,**b**) TEM images of the OPS nanoparticles.

3.2. Interlaminar Shear Strength

As shown in Figure 5, the effect of OPS particles on the interlaminar shear characteristics of hybrid composites under room temperature was investigated. It was discovered that the shear parameters including ILSS strength and shear modulus rose with increasing particle concentration up to 4 wt.% and afterward dropped. The ILSS strength (38.10 MPa) and shear modulus of hybrid composites without nanoparticles were the lowest (0.97 GPa). On the other hand, incorporating OPS fillers into the hybrid composite enhanced the interlaminar shear strength and shear modulus [27]. The greatest ILSS strength (47.28 MPa) and shear modulus (1.56 GPa) were obtained when 4 wt.% OPS fillers were encumbered into the hybrid materials. This finding showed that accumulating fillers to polymeric materials improved the ILSS characteristics by snowballing the superficial zone, energy absorption capabilities, and limiting voids along the composite laminate [28]. This suggests that incorporating 4 wt.% filler into the OPS nanoparticles improved the epoxy's capacity to transfer and distribute stress to the desired level. Furthermore, this scenario was most likely caused by the homogeneous scattering of palm shell fillers in the resin, which consequently resulted in enhanced matrix/filler connections and fiber surface expanse. Consequently, stress transmission became more straightforward, and the sample could withstand a more significant load, leading to higher ILSS for the composite samples. Homogeneous particle distribution improved the filler–matrix interactions and fiber interface adhesion, leading to increased energy retention. The reduction in mechanical performance with an increment in the OPS nanoparticles from 4% to 6% was due to the aggregation of nanoparticles with the maximum loading, which affects the stress transmission and results in poor wettability of the biopolymers [29].

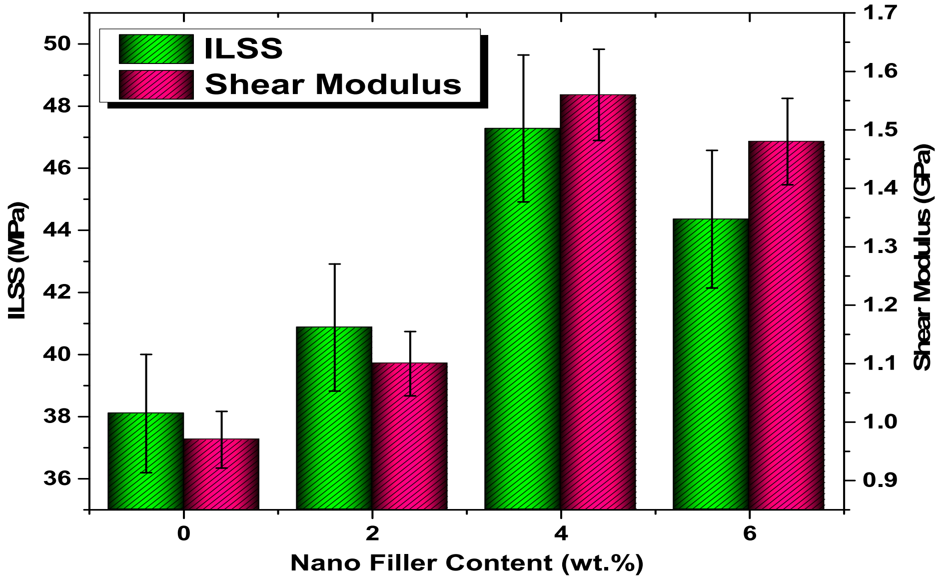

Figure 5. The ILSS and shear modulus of flax/OPS nanofiller/epoxy-based hybrid composites under room temperature.

The ILSS and their shear modulus of polymeric materials after different cryogenic healing durations are shown in Figure 6a,b. In cryogenic processing, the composite plates are exposed to liquid N_2 at −196 °C and thermally cycled. The composites were visible, with 15 min of cryogenic treatment demonstrating their good mechanical results. This might be related to the cryogenic exertion of the composite materials, which produces residual stress at compressive contact [30]. The changing matrix and fiber shrinkage create such residual strains at low temperatures. Because the fiber has a lower thermal expansivity than the polymer matrix, the resultant stresses are compressive in the fiber and tensile in the matrix. These interfacial compression stresses keep the fiber and polymer interacting and enhance the adherence, resulting in better outcomes [31].

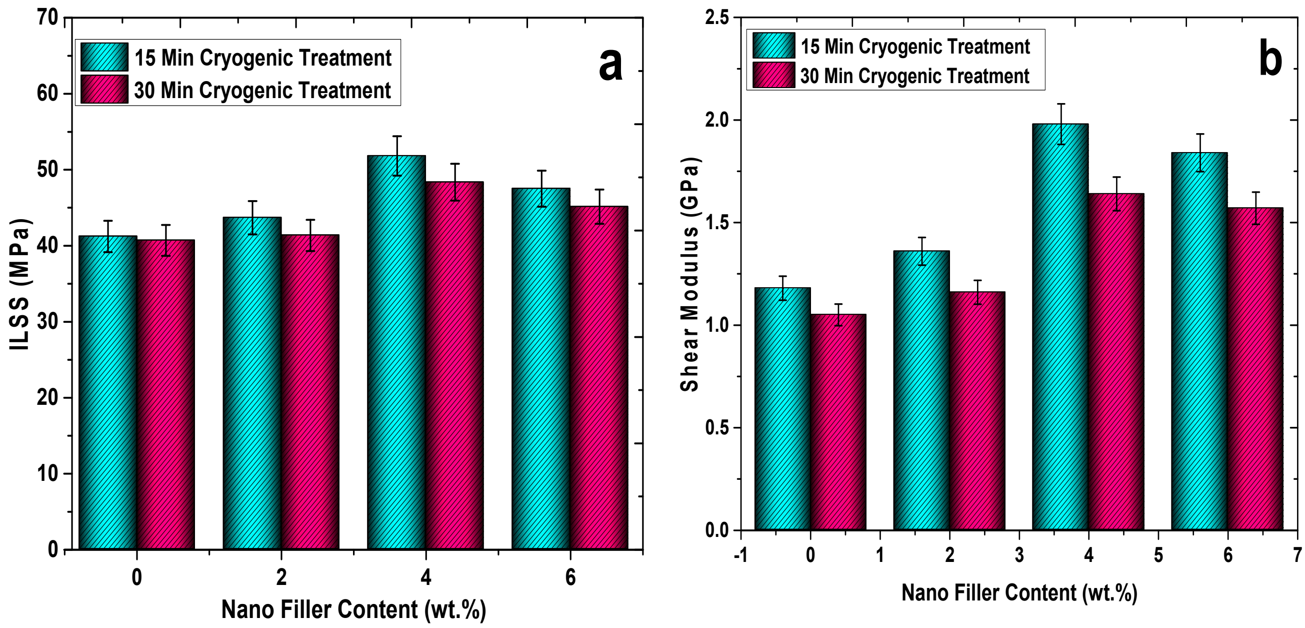

Figure 6. The ILSS and shear modulus of the flax/OPS nanofiller/epoxy based hybrid composites under cryogenic conditions. (**a**) Nano filler content vs. ILSS; (**b**) Nano filler content vs. shear modulus.

The ILSS behavior of hybrid composites was lowered when the samples were processed for longer than 15 min. Because the matrix-reinforcement enhancement was mismatched, the lengthier liquid nitrogen habituation period provided the highest stress in terms of heat. Delamination processes are much more detrimental to nanoscale fillers and flax hybrid-epoxy frameworks due to the decreased contact. This might be because it significantly reduces the time it takes to cure the epoxy matrix [32]. Poor-adherence composite properties showed significant interfacial delamination zones, intensifying the failure issues that could cause the composite to rupture. Given the variations in the heat conductance between the matrix and fiber, greater internal forces formed for the nanocomposites handled beyond 15 min, which were released by physical progressions such as voids, matrix/fiber interfacial delamination, cracks, etc. The SEM images (Figure 7) indicate the above findings [33]. Figure 7c–f shows the microstructural images of various concentrations of OPS fillers such as 0 wt.%, 2 wt.%, 4 wt.%, and 6 wt.% at 30 min of cryogenic treatment.

3.3. Storage Modulus

The impact of the nanofiller concentration on the storage modulus (S) of the flax/epoxy nanocomposite is shown in Figure 8. The storage modulus S was observed to be lowered with temperatures throughout all instances when evaluating the fluctuations of S with temperatures of the flax/epoxy composites. Figure 8 shows that the S tends to become wider throughout the glassy zone because the elements are closer together, closely packed, and frozen, resulting in a higher stored modulus value under Tg. Furthermore, at 80–90 °C, the S curve showed a sharp dip, suggesting a glass/rubbery sequence. However, whenever the temperature was raised, the composite constituents displayed more significant intermolecular interaction and thus lost their close-packed configuration, lowering the S levels in the stretchy area. On the other hand, the unfilled and filler-filled hybrid composites showed no significant modifications in the flexible area.

The storage modulus graphs also showed that adding nanofiller to the flax/epoxy composites significantly increased the S values. Combining the nanofiller efficiently reduced the modulus difference between the stiff flax fibers and matrix materials [34]. According to Figure 8, for all flax-OPS fractions examined, an increase in the storage modulus with the OPS filler concentration was found over the whole temperature range. According to

Ornaghi et al. [35], this improvement is due to the high barriers imposed by the flax fibers on the polymer, increasing the stress transmission at the fiber interface. Another aspect that might boost the S is the interaction of nearby chains because the relaxing process requires more molecule collaboration. Romanzine et al. [36] studied ramie materials and found that enhancing the overall fiber quantity improved the resin's capacity to allow mechanical restrictions while recovering the viscoelastic displacement. As a result, the rigidity of the composites increased as the filler concentration increased.

The effectiveness factor (C) was computed for each weight % of the OPS filler particles by using Equation (1). This investigation showed C values of 0.10, 0.09, and 0.088 for the 2 wt.%, 4 wt.%, and 6 wt.% OPS filler particles, respectively. Idicula et al. [37] investigated the reinforcement effectiveness of the banana/sisal/polyester composites. They reported a minimum C value at 40% fiber volume fraction, justified by the extreme fiber-to-fiber interaction that appeared with higher fiber loading, reducing the effective stress transfer between the fibers and matrix. The lowest number obtained in this experiment was 6 wt.%, and the presence of a minimal could not be confirmed since the weight percentage was unable to be elevated over 6% due to the molding limits.

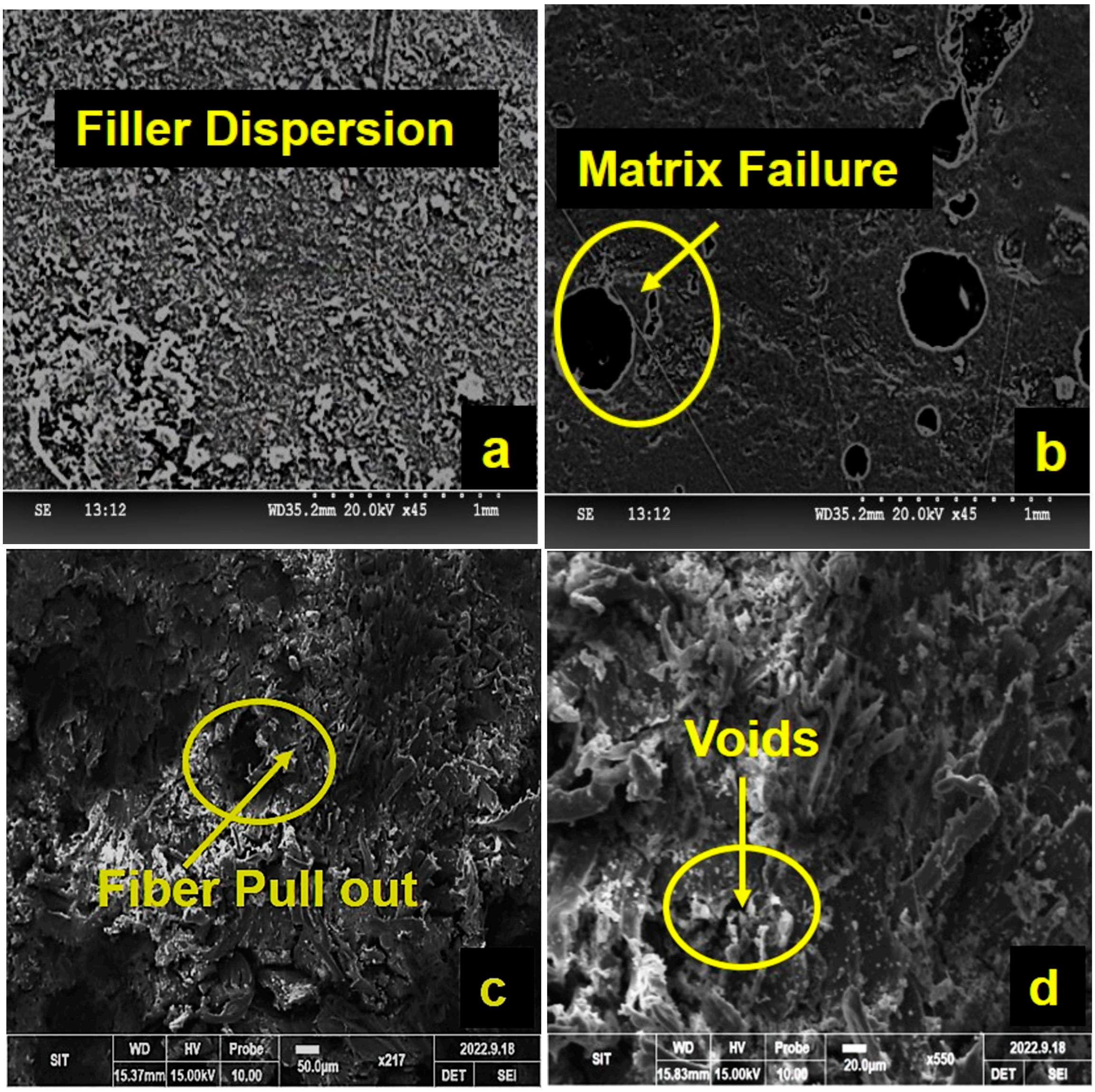

Figure 7. *Cont.*

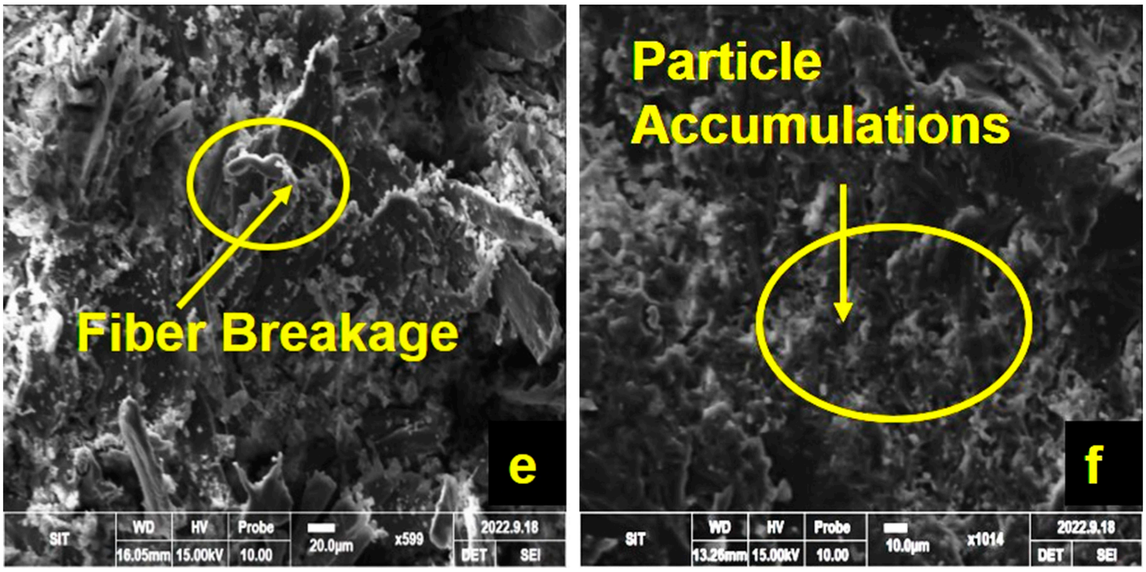

Figure 7. Microstructural examination of the 4% OPS filler/flax/epoxy based hybrid composites under aa (**a**) 15 min and (**b**) 30 min cryogenic environment; (**c**) 0 wt.% OPS; (**d**) 2 wt.% OPS; (**e**) 4 wt.% OPS; and (**f**) 6 wt.% of OPS based ILSS composite after fracture at 30 min cryogenic treatment.

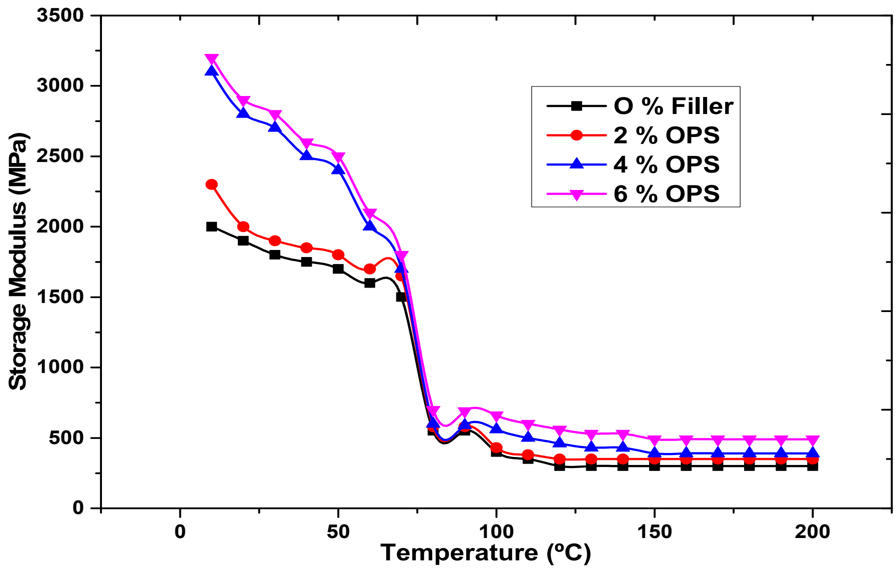

Figure 8. Effectiveness of the OPS nanofiller content on the flax/epoxy-based hybrid composites on the storage modulus.

3.4. Loss Modulus

Figure 9 shows the combined DMA loss modulus (S′) against the temperature graphs of the unfilled and filler-filled hybrid composites. Incorporating 2 wt.% OPS nanofiller into the flax/epoxy composites improved the loss modulus, which showed a consistent trend in the storage modulus graph. However, due to the polymerization's free mobility, all loss modulus contours achieved the most significant benefit for the maximum mechanical power dissipation and decreased for extreme temperatures [38]. Figure 8 further shows that the addition of micro-OPS leads to a widening of the loss modulus peaks due to the high number of crosslinks. The optimum elevation of the S′ values was much more significant for all of the flax/epoxy hybrid nanocomposites compared to the flax/epoxy composites due to the rise in frictional resistance, which improved the energy dissipation.

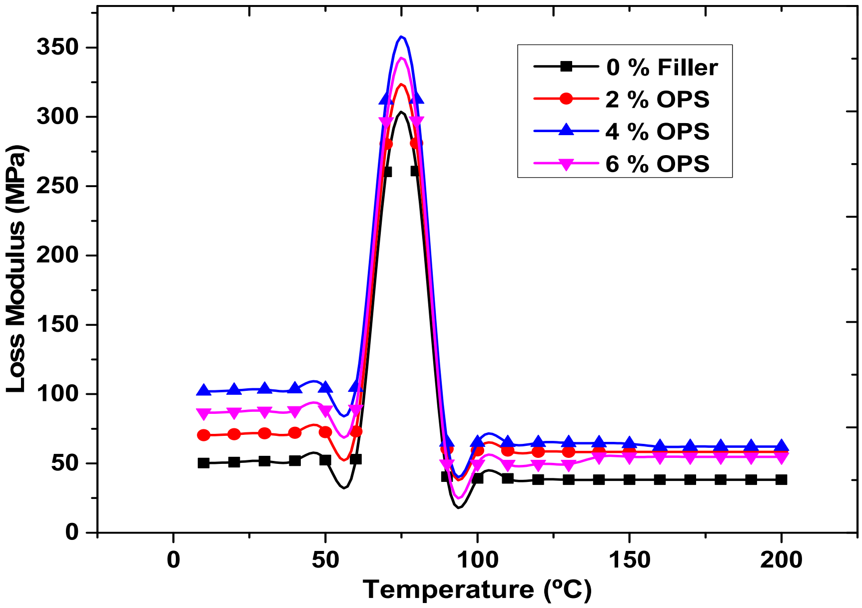

Figure 9. Effectiveness of the OPS nanofiller content on the flax/epoxy-based hybrid composites on the loss modulus.

The rise in both the storage (S) and loss (S′) modulus standards with the addition of palm shell filler could be addressed [32]. As a result, the S′ peak height of the flax/epoxy composites was smaller, but the S′ maximum amplitude of the 4 wt.% OPS/flax/epoxy hybrid nanocomposites was greater. The 4 wt.% OPS/flax/epoxy hybrid nanocomposites had substantially higher S′ values in the transition zone than the 6% nano-OPS/flax/epoxy and 2 wt.% nano OPS/flax/epoxy composites. The ionic and non-ionic assemblies of nano-OPS improved the interference bonding among reagents, resulting in an S value enhancement. However, the 2 wt.% and 6 wt.% filled nano-OPS/flax/epoxy hybrid nanocomposites presented significantly greater dynamic loss modulus values than the 2 wt.% nano-OPS/flax/epoxy hybrid nanocomposites. Furthermore, when OPS fillers (2 wt.% nano OPS, 4 wt.% OPS and 6 wt.% OPS) were added to the flax-based composites, the complex modulus (S′) of the resultant nanofiller filled composite was enhanced compared to the unfilled composites.

3.5. Damping Factor

A mechanical damping factor was indicated by tan α. It is the ratio of the dynamic loss modulus (s) to the dynamic storage modulus (S′) that may be used to predict the occurrence of molecular mobility transitions such as the glass transition temperature (Tg). Tg was greater in models with more limitations and a higher degree of reinforcement, as per Almeida et al. [24]. Tg improved from 70 °C to 75–87 °C when the flax and epoxy resin-based composites were compared, but no significant difference in Tg was found across the combinations. Figure 10 depicts the tan alpha curves for all composites. The inclusion of OPS fillers reduced the tan alpha peak due to the higher limitations in the mobility of the polymer molecules induced by the presence of fillers and stiff fibers. Whenever the filler quantity is modest, there can be places in the composite with a heavy proportion of resin (matrix) that is untouched by the inclusion of fibers [39]. The glass transition temperature calculated from the tan alpha curve showed no discernible trend. All Tg values for the composites were within the range of 75–87 °C, which was the same as the Tg for the epoxy and flax-based composites (75 °C). As a result, the addition of OPS fillers had a greater impact on the tan alpha peak than on the reported glass transition temperature. Pothan et al. [40] found that composites with a poor fiber–matrix interface wasted more energy than composites with strong interface bonding, implying that increased damping suggests lower interfacial interaction. The increase in filler content resulted in a reduction in the tan alpha peak in Figure 8, as the total interfacial surface inside the compound increased. The interface adherence was calculated from the tan alpha peak height measurements using the methods provided by Correa et al. [41]. According to these researchers, molecule mobility around the reinforcements was decreased for high interface adhesion, while lower tan α values indicated enhanced interactions at the matrix–fiber interface [42].

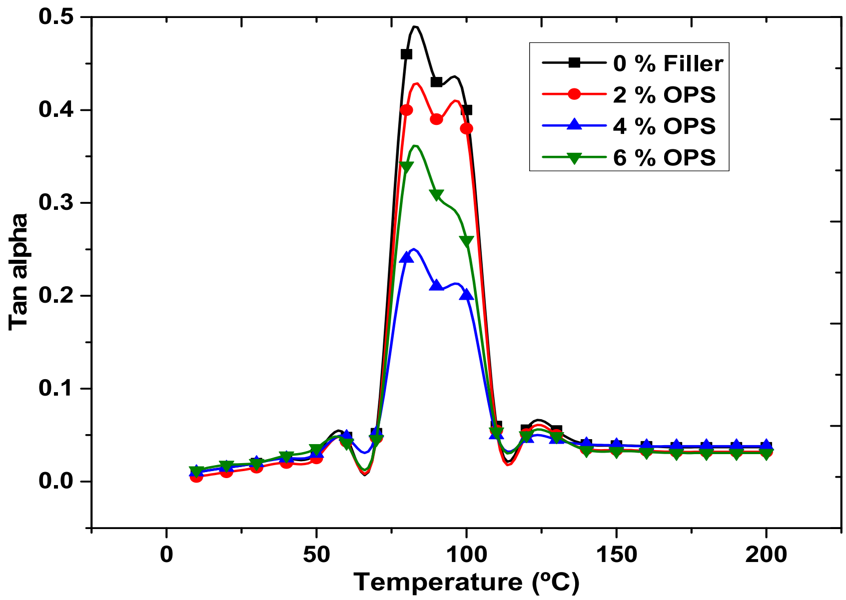

Figure 10. The effectiveness of OPS nanofiller content on the flax/epoxy-based hybrid composites on the damping factor.

4. Conclusions

The ball milling procedure was effective in producing OPS nanoparticles from OPS. Palm shell particles were used as a filler to progress the ILSS and dynamic characteristics of the usual fabric strengthened hybrid polymeric materials in this work. According to the findings, the OPS nanomaterials can be used as organic instead of artificial fillers. Furthermore, loading a 4 wt.% OPS filler into organic fibers strengthened the epoxy polymeric materials and resulted in the best ILSS and dynamic properties. Hybrid composites can also benefit from cryogenic treatment to improve their ILSS behavior. This might be because of the lingering tension caused by the composite material's compression interaction due to cryogenic straining. Changes in the matrices and fiber shrinkage caused strain to arise at cold temperatures. When specimens were handled for more than 15 min, the ILSS features of the composites diminished. More extended cryogenic conditioning periods might result in superior thermal conductance due to the growing fiber–resin mismatch. The storage and loss modulus of the flax/epoxy composites were improved by adding a 4 wt.% OPS nanofiller. The hardness and stiffness of the added OPS nanofiller can be attributed to the improvement.

In comparison to the flax/epoxy composites, the damping factor of the 4 wt.% nano-OPS/flax/epoxy hybrid nanocomposite was noticeably lower. The reduction in the damping factor can be attributed to the OPS nanofiller's limitation of the epoxy molecular chain's free segmental mobility and better interfacial adhesion among the flax fibers and epoxy matrix. When 4 wt.% OPS nanoparticles were loaded into the composites, the SEM examination indicated the presence of fiber pulling out, voids, and fiber breakage. However, with the 4 wt.% OPS nanoparticle loading into the hybrid composites, this limited mismatch among the nanoparticles and matrices may be solved by contacting the fiber with a compatibilizer.

Author Contributions: Conceptualization: N.L.; Data curation: N.L. and S.K.; Formal analysis: S.K. and V.G.; Funding acquisition: S.C. (Shahariar Chowdhury) and S.C. (Sittiporn Channumsin); Investigation: S.C. (Sittiporn Channumsin), M.C., K.T. and J.A.D.; Methodology: N.L.; Project administration: S.C. (Sittiporn Channumsin), M.C. and K.T.; Resources: V.G. and P.P.P.; Software: J.A.D. and P.P.P.; Supervision: M.C., S.C. (Sittiporn Channumsin), C.S. and T.W.; Validation: T.W.; Visualization: C.S.; Writing—original draft: N.L. and S.K.; Writing—review & editing: S.C. (Shahariar Chowdhury), M.C., J.A.D. and C.S. All authors have read and agreed to the published version of the manuscript.

Funding: This research was supported by Prince of Songkla University by grant number ENV6502112N. This work was also funded by the Geo-Informatics and Space Technology Development Agency (Public Organization)—GISTDA.

Institutional Review Board Statement: Not applicable.

Informed Consent Statement: Not applicable.

Data Availability Statement: Not applicable.

Conflicts of Interest: The authors declare no conflict of interest.

References

1. Li, Z.; Wang, X.; Wang, L. Properties of Hemp Fibre Reinforced Concrete Composites. *Compos. Part A Appl. Sci. Manuf.* **2006**, *37*, 497–505. [CrossRef]
2. Ramesh, M.; Palanikumar, K.; Reddy, K.H. Comparative Evaluation on Properties of Hybrid Glass Fiber-Sisal/Jute Reinforced Epoxy Composites. *Procedia Eng.* **2013**, *51*, 745–750. [CrossRef]
3. Aarti, C. A Review on Pharmacological and Biological Properties of Calotropis Gigantea. *Int. J. Recent Sci. Res.* **2014**, *5*, 716–719.
4. Mishra, S.; Mohanty, A.K.; Drzal, L.T.; Misra, M.; Parija, S.; Nayak, S.K.; Tripathy, S.S. Studies on Mechanical Performance of Biofibre/Glass Reinforced Polyester Hybrid Composites. *Compos. Sci. Technol.* **2003**, *63*, 1377–1385. [CrossRef]
5. dos Santos, J.C.; Siqueira, R.L.; Vieira, L.M.G.; Freire, R.T.S.; Mano, V.; Panzera, T.H. Effects of Sodium Carbonate on the Performance of Epoxy and Polyester Coir-Reinforced Composites. *Polym. Test.* **2018**, *67*, 533–544. [CrossRef]
6. Rana, A.K.; Mandal, A.; Mitra, B.C.; Jacobson, R.; Rowell, R.; Banerjee, A.N. Short Jute Fiber-Reinforced Polypropylene Composites: Effect of Compatibilizer. *J. Appl. Polym. Sci.* **1998**, *69*, 329–338. [CrossRef]
7. Al-Oqla, F.M.; Sapuan, S.M. Natural Fiber Reinforced Polymer Composites in Industrial Applications: Feasibility of Date Palm Fibers for Sustainable Automotive Industry. *J. Clean. Prod.* **2014**, *66*, 347–354. [CrossRef]
8. Öztürk, S. Effect of Fiber Loading on the Mechanical Properties of Kenaf and Fiberfrax Fiber-Reinforced Phenol-Formaldehyde Composites. *J. Compos. Mater.* **2010**, *44*, 2265–2288. [CrossRef]
9. Ashori, A.; Bahreini, Z. Evaluation of Calotropis Gigantea as a Promising Raw Material for Fiber-Reinforced Composite. *J. Compos. Mater.* **2009**, *43*, 1297–1304. [CrossRef]
10. Sumesh, K.R.; Kanthavel, K. Green Synthesis of Aluminium Oxide Nanoparticles and Its Applications in Mechanical and Thermal Stability of Hybrid Natural Composites. *J. Polym. Environ.* **2019**, *27*, 2189–2200. [CrossRef]
11. Giuliani, P.M.; Giannini, O.; Panciroli, R. Characterizing Flax Fiber Reinforced Bio-Composites under Monotonic and Cyclic Tensile Loading. *Compos. Struct.* **2022**, *280*, 114803. [CrossRef]
12. Woigk, W.; Nagel, Y.; Gantenbein, S.; Coulter, F.B.; Masania, K.; Studart, R. Flax-Based Natural Composites Hierarchically Reinforced by Cast or Printed Carbon Fibres. *Compos. Sci. Technol.* **2022**, *226*, 109527. [CrossRef]
13. Pregi, E.; Faludi, G.; Kun, D.; Móczó, J.; Pukánszky, B. Three-Component Polypropylene/Lignin/Flax Composites with High Natural Additive Content for Structural Applications. *Ind. Crops Prod.* **2022**, *182*, 114890. [CrossRef]
14. Alamri, H.; Low, I.M. Effect of Water Absorption on the Mechanical Properties of N-SiC Filled Recycled Cellulose Fibre Reinforced Epoxy Eco-Nanocomposites. *Polym. Test.* **2012**, *31*, 810–818. [CrossRef]
15. Asim, M.; Abdan, K.; Jawaid, M.; Nasir, M.; Dashtizadeh, Z.; Ishak, M.R.; Hoque, M.E.; Deng, Y. A Review on Pineapple Leaves Fibre and Its Composites. *Int. J. Polym. Sci.* **2015**, *2015*, 950567. [CrossRef]
16. Sheikh Md Fadzullah, S.H.; Mustafa, Z. Fabrication and Processing of Pineapple Leaf Fiber Reinforced Composites. In *Green Approaches to Biocomposite Materials Science and Engineering*; IGI Global: Hershey, PA, USA, 2016; pp. 125–147. [CrossRef]
17. Adeniyi, A.G.; Onifade, D.V.; Ighalo, J.O.; Adeoye, A.S. A Review of Coir Fiber Reinforced Polymer Composites. *Compos. Part B Eng.* **2019**, *176*, 107305. [CrossRef]
18. Khan, R.A.; Khan, M.A.; Zaman, H.U.; Pervin, S.; Khan, N.; Sultana, S.; Saha, M.; Mustafa, A.I. Comparative Studies of Mechanical and Interfacial Properties between Jute and E-Glass Fiber-Reinforced Polypropylene Composites. *J. Reinf. Plast. Compos.* **2010**, *29*, 1078–1088. [CrossRef]
19. Mishra, S.; Misra, M.; Tripathy, S.S.; Nayak, S.K.; Mohanty, A.K. Potentiality of Pineapple Leaf Fibre as Reinforcement in PALF-Polyester Composite: Surface Modification and Mechanical Performance. *J. Reinf. Plast. Compos.* **2001**, *20*, 321–334. [CrossRef]

20. Ghosh, S.; Das, A.P. Modified Titanium Oxide (TiO2) Nanocomposites and Its Array of Applications: A Review. *Toxicol. Environ. Chem.* **2015**, *97*, 491–514. [CrossRef]
21. Singh, T.; Gangil, B.; Ranakoti, L.; Joshi, A. Effect of Silica Nanoparticles on Physical, Mechanical, and Wear Properties of Natural Fiber Reinforced Polymer Composites. *Polym. Compos.* **2021**, *42*, 2396–2407. [CrossRef]
22. Dey, T.K.; Hossain, A.; Jamal, M.; Layek, R.K.; Uddin, M.E. Zinc Oxide Nanoparticle Reinforced Waste Buffing Dust Based Composite Insole and Its Antimicrobial Activity. *Adv. Polym. Technol.* **2022**, *2022*, 7130551. [CrossRef]
23. Nam, T.H.; Ogihara, S.; Tung, N.H.; Kobayashi, S. Effect of Alkali Treatment on Interfacial and Mechanical Properties of Coir Fiber Reinforced Poly(Butylene Succinate) Biodegradable Composites. *Compos. Part B Eng.* **2011**, *42*, 1648–1656. [CrossRef]
24. Velmurugan, G.; Siva Shankar, V.; Natrayan, L.; Sekar, S.; Patil, P.P.; Kumar, M.S.; Thanappan, S. Multiresponse Optimization of Mechanical and Physical Adsorption Properties of Activated Natural Fibers Hybrid Composites. *Adsorpt. Sci. Technol.* **2022**, *2022*. [CrossRef]
25. Materials, C.N. Tutorial on Powder X-Ray Di Ff Raction for Characterizing Nanoscale Materials. *ACS Nano* **2019**, *13*, 7359–7365. [CrossRef]
26. Kutvonen, A.; Rossi, G.; Puisto, S.R.; Rostedt, N.K.J.; Ala-nissila, T.; Kutvonen, A.; Rossi, G.; Puisto, S.R.; Rostedt, N.K.J. Influence of Nanoparticle Size, Loading, and Shape on the Mechanical Properties of Polymer Nanocomposites Influence of Nanoparticle Size, Loading, and Shape on the Mechanical Properties of Polymer Nanocomposites. *J. Chem. Phys.* **2012**, *137*, 214901. [CrossRef]
27. Ganesan, V.; Kaliyamoorthy, B. Utilization of Taguchi Technique to Enhance the Interlaminar Shear Strength of Wood Dust Filled Woven Jute Fiber Reinforced Polyester Composites in Cryogenic Environment. *J. Nat. Fibers* **2020**, *19*, 1990–2001. [CrossRef]
28. Amin, F.; Khattak, B.; Alotaibi, A.; Qasim, M.; Ahmad, I.; Ullah, R.; Bourhia, M.; Gul, A.; Zahoor, S.; Ahmad, R. Green Synthesis of Copper Oxide Nanoparticles Using Aerva Javanica Leaf Extract and Their Characterization and Investigation of In Vitro Antimicrobial Potential and Cytotoxic Activities. *Evid. Based Complement. Alternat. Med.* **2021**, *2021*, 5589703. [CrossRef]
29. Edayadulla, N.; Basavegowda, N.; Lee, Y.R. Journal of Industrial and Engineering Chemistry Green Synthesis and Characterization of Palladium Nanoparticles and Their Catalytic Performance for the Ef Fi Cient Synthesis of Biologically Interesting Di (Indolyl) Indolin-2-Ones. *Korean Soc. Ind. Eng. Chem.* **2014**, *21*, 1365–1372. [CrossRef]
30. Velmurugan, G.; Babu, K. Statistical Analysis of Mechanical Properties of Wood Dust Filled Jute Fiber Based Hybrid Composites under Cryogenic Atmosphere Using Grey-Taguchi Method. *Mater. Res. Express* **2020**, *7*, 065310. [CrossRef]
31. Sanyahumbi, D.; Yong, P.; Macaskie, L.E. Biorecovered Precious Metals from Industrial Wastes : Single-Step Conversion of a Mixed Metal Liquid Waste to a Bioinorganic Catalyst with Environmental Application. *Environ. Sci. Technol.* **2006**, *40*, 1015–1021.
32. Li, S.; Deng, D.; Shi, Q.; Liu, S. Electrochemical Synthesis of a Graphene Sheet and Gold Nanoparticle-Based Nanocomposite, and Its Application to Amperometric Sensing of Dopamine. *Microchimica Acta* **2012**, *177*, 325–331. [CrossRef]
33. Daté, M.; Okumura, M.; Tsubota, S.; Haruta, M. Vital Role of Moisture in the Catalytic Activity of Supported Gold Nanoparticles. *Angew. Chem.* **2004**, *116*, 2181–2184. [CrossRef]
34. Yusoff, N.; Pandikumar, A.; Ramaraj, R. Gold Nanoparticle Based Optical and Electrochemical Sensing of Dopamine. *Microchim. Acta* **2015**, *182*, 2091–2114. [CrossRef]
35. Ornaghi, H.L.; Bolner, A.S.; Fiorio, R.; Zattera, A.J.; Amico, S.C. Mechanical and Dynamic Mechanical Analysis of Hybrid Composites Molded by Resin Transfer Molding. *Appl. Polym.* **2010**, *118*, 887–896. [CrossRef]
36. Romanzini, D.; Lavoratti, A.; Ornaghi, H.L.; Amico, S.C.; Zattera, A.J. Influence of Fiber Content on the Mechanical and Dynamic Mechanical Properties of Glass/Ramie Polymer Composites. *Mater. Des.* **2013**, *47*, 9–15. [CrossRef]
37. Idicula, M.; Malhotra, S.K.; Joseph, K.; Thomas, S. Dynamic Mechanical Analysis of Randomly Oriented Intimately Mixed Short Banana/Sisal Hybrid Fibre Reinforced Polyester Composites. *Compos. Sci. Technol.* **2005**, *65*, 1077–1087. [CrossRef]
38. Mikami, Y.; Dhakshinamoorthy, A.; Alvaro, M.; Garcia, H. Catalytic activity of unsupported gold nanoparticles. *Catal. Sci. Technol.* **2013**, *1*, 58–69. [CrossRef]
39. Abbasi, S.; Hekmati, M. Functionalization of Multi—Walled Carbon Nanotubes with Pramipexole for Immobilization of Palladium Nanoparticles and Investigation of Catalytic Activity in the Sonogashira Coupling Reaction. *Appl. Organomet. Chem.* **2016**, *31*, e3600. [CrossRef]
40. Pothan, L.A.; Oommen, Z.; Thomas, S. Dynamic Mechanical Analysis of Banana Fiber Reinforced Polyester Composites. *Compos. Sci. Technol.* **2003**, *63*, 283–293. [CrossRef]
41. Correa, C.A.; Razzino, C.A.; Hage, E. Role of Maleated Coupling Agents on the Interface Adhesion of Polypropylene—Wood Composites. *J. Thermoplast. Compos. Mater.* **2007**, *20*, 323–339. [CrossRef]
42. Borah, R.K.; Saikia, H.J.; Mahanta, A.; Das, V.K.; Bora, U.; Thakur, A.J. Biosynthesis of poly(ethylene glycol)-supported palladium nanoparticles using *Colocasia esculenta* leaf extract and their catalytic activity for Suzuki–Miyaura cross-coupling reactions. *RSC Adv.* **2015**, *5*, 72453–72457. [CrossRef]